A global seismic model as proxy for surface heat flux: Application to Antarctica

Nikolai M. Shapiro and Michael H. Ritzwoller
Center for Imaging the Earth's Interior

Department of Physics, University of Colorado

Campus Box 390, Boulder, CO 80309, USA (e-mail: nshapiro@ciei.colorado.edu)

Submitted to *Earth and Planetary Science Letters*, March 25, 2003.

Short title: SEISMIC MODEL AND SURFACE HEAT FLUX

Abstract.

We present a method that uses a global seismic model of the crust and upper mantle to guide the smoothing and interpolation of heat flow measurements where they exist and the extrapolation of existing measurements to regions where such measurements are rare or absent. For any chosen spatial point on the globe the procedure generates a heat flow value as a weighted average over all regions where heat flow data are available that are structurally similar to the target point. The weights in the average are based on a "structural similarity functional" which we introduce to quantify the structural analogy between different regions. We apply this procedure world-wide using the global heat flow data base of Pollack et al. [1] guided by an update of the 3-D shear velocity model of the crust and uppermost mantle of Shapiro and Ritzwoller [2]. Particular attention is drawn to surface heat flow maps of Antarctica, because these maps are needed to understand the dynamics of Antarctic ice sheets. It is noteworthy that heat flow in West Antarctica may be nearly three times higher than in East Antarctica. This high heat flow may contribute to the instability of the West Antarctic Ice Sheet.

Introduction

The dynamics of the Antarctic Ice Sheet is largely controlled by fast moving ice streams [3, 4] whose efficiency is affected by the lubricating effect of water in a weak basal layer. The melting/freezing rate at the bottom of the ice depends on the sub-glacial geological conditions, including sub-glacial geothermal flux [5, 6, 7]. Unfortunately, heat flow information across Antarctica is exceedingly rare. A full understanding of the behavior of the Antarctic Ice Sheet and of its role in global climate change, therefore, will require better knowledge of the geothermal flux across Antarctica.

There are thousands of heat flow measurements that have been obtained in a variety of tectonic regimes both within continents and oceans [1]. The distribution of these observations, however, is very inhomogeneous, having been obtained dominantly in the Northern hemisphere within North America and Europe (Figure 1). The measurement of heat flow at the base of the Antarctic ice sheets is technically challenging and the accumulation of direct heat flow observations across Antarctica will be slow.

Our purpose is to apply information about heat flow acquired in other regions of the world in a meaningful way to Antarctica. There are several possible approaches to this. One method would be to use a tectonic regionalization, to summarize known heat flow information by tectonic type, and then apply the results to Antarctica. Rough regionalizations have been used to produce characteristic heat flow values for continental tectonic regimes [1, 8, 9, 10] and in oceans average heat flow has been computed as a function of sea-floor age [11, 12]. This approach is not ideal for Antarctica because Antarctic tectonics is not well understood. A second method that has some merit would be to predict heat flow directly from a 3-D seismic model. The merit derives from the fact that the vertical seismic velocity gradient in the mantle is related to the temperature gradient which control the mantle component of heat flow [13, 14, 15, 16]. Demerits include the necessity of introducing the crustal contribution to heat flow through the decay of radioactive elements in some way, the fact that heat flow information from elsewhere in the world would not be explicitly utilized, and the confounding effects of

composition, mantle volatiles, and anelasticity. Shapiro and Ritzwoller [16] argue that for seismic models to predict the mantle component of heat flow faithfully would require the imposition of physical constraints on the inversion which have not yet been applied systematically.

Our goal is to merge these two alternative methods in a way that will accentuate their strengths and minimize their weaknesses. Our approach is to use structural, as opposed to tectonic, analogies between parts of Antarctica and regions elsewhere in the world where heat flow measurements are available. The structural analogies are defined by a recent 3-D seismic model of the crust and uppermost mantle and guide the extrapolation of heat flow information from elsewhere in the world to Antarctica. The principal advantages of our approach are that the global seismic model provides a uniform description of the Earth and the concept of structural similarity is formalizable and allows future extension. This has allowed us to develop a completely automated algorithm to extrapolate existing heat flow data over the whole globe and to produce heat flow maps for regions in which direct heat flow measurements are entirely absent.

The seismic model and structural similarity

Seismic models based on surface waves are most suitable to establish structural similarities between different parts of the Earth because they provide a relatively homogeneous coverage over the whole Earth and relatively good resolution in the crust and in the uppermost mantle, the layers most directly related to surface heat flux. We use an update of the 3-D shear velocity model of Shapiro and Ritzwoller [2]. The data used to construct this model consist of a large set of dispersion curves for broad-band Rayleigh and Love wave group [17, 18] and phase [19, 20] velocities. Period-specific dispersion maps were constructed with "diffraction tomography" which is based on a physical model of the surface wave lateral sensitivity kernels [21]. These dispersion maps are subjected to a non-linear Monte-Carlo inversion that produces an ensemble of acceptable shear-velocity models at all points on a $2^\circ \times 2^\circ$ geographical grid world-wide

[2].

Three features of this model make it particularly appropriate to establish structural similarity world-wide. First, the large number of short-period group-velocity measurements used in the construction of this model improves the vertical resolution of the model significantly compared to traditional surface-wave models based on phase-velocity measurements alone. Second, this model is based on a particularly large data set of surface-wave paths across Antarctica [18]. Third, because the model is based on a Monte-Carlo inversion, it has uncertainties, which we will need in the following.

We quantify the concept of structural similarity between to locations x_1 and x_2 by introducing the "structural similarity functional", $S(x_1, x_2)$. Although its definition is ad-hoc, the functional must satisfy certain conditions. For example, two points must be deemed perfectly similar when the shear velocity profiles directly beneath these points are identical and the points must be dissimilar when the corresponding profiles differ significantly. Here, we define the similarity functional as composed of two terms:

$$S(x_1, x_2) = \frac{1}{2}\left(S^{\beta}(x_1, x_2) + S^{moho}(x_1, x_2)\right). \tag{1}$$

The first term $S^{\beta}(x_1, x_2)$ is the weighted difference between the shear velocity profiles at points x_1 and x_2, $\beta_1(z)$ and $\beta_2(z)$:

$$S^{\beta}(x_1, x_2) = \frac{\int_{z_1}^{z_2} w(z)\left(\frac{|\beta_2(z)-\beta_1(z)|}{u(z)}\right) dz}{\int_{z_1}^{z_2} w(z) dz}, \tag{2}$$

where z is depth, the limits of the integral are 0 km and 300 km, $u(z)$ is the global average uncertainty of the seismic model estimated with the Monte-Carlo inversion, and $w(z)$ is a depth-dependent weight function. Figure 2a shows the depth-dependent weight function and Figure 2b shows the estimated average uncertainty in the shear velocity model. As a result of these choices, the term $S^{\beta}(x_1, x_2)$ is dominated by the mantle part of the model. The second term $S^{moho}(x_1, x_2)$ is introduced to account for differences in crustal thickness between points x_1 and x_2, Z_1^{moho} and Z_2^{moho}:

$$S^{moho}(x_1, x_2) = \frac{|Z_1^{moho} - Z_2^{moho}|}{\sigma_{moho}}. \tag{3}$$

We use $\sigma_{moho} = 10$ km, which effectively discriminates between oceanic and continental crust.

If $S(x_1, x_2) < 1$, the depth-averaged difference between the two shear velocity profiles is smaller than the average uncertainty in the model, so the points x_1 and x_2 are considered to be similar. When $S(x_1, x_2) > 1$, the difference between the profiles is deemed significant and the two points are not considered to be similar. Figures 2c and 2d display maps of the similarity functional for two points in Antarctica. The one in East Antarctica (84S, 90E) is similar to old cratonic regions (e.g., Canadian craton, East-European platform, Siberian craton, West-African craton) consistent with tectonic reconstructions showing East Antarctica to be a fragment of the old supercontinents Rodinia and Gondwana [22, 23]. West Antarctic tectonics is dominated by the West Antarctic Rift System [24, 5, 25, 26]. Therefore, it is not surprising that the similarity functional identifies the point in West Antarctica (78S, 110W) to be similar to continental regions with relatively young extensional tectonics (e.g., Western North America, Iceland, Red Sea, Eastern Turkey, Western Mediterranean).

Estimated heat flow maps

We use the global heat flow compilation of Pollack et al. [1] as our primary data set. Figure 1 identifies the measurement locations and Figure 3 shows the variability of the measurements (rms = 55 mW/m^2). The extrapolation procedure is based on the similarity functional in the following way. For each target point x_0 where we wish to extrapolate a heat flow value, the similarity functional $S(x_0, x)$ defines the regions with similar seismic structure (as shown in Figures 2c and 2d). The heat flux is computed as the average of the heat flow measurements within those regions of similarity. This is formally performed by introducing a similarity-based weight function:

$$W(S) = \exp\left(-\frac{S^2}{2\sigma_S^2}\right) \tag{4}$$

where σ_S is a free parameter defining the degree of smoothing (in this paper, we use $\sigma_S = 0.2$). The average heat flux $H(x_0)$ and its standard deviation $\sigma_H(x_0)$ at point x_0 are computed as the weighed sum over all heat flow measurements world-wide obtained at locations x_n, where the weights derive from equation (4):

$$H(x_0) = \frac{\sum_n W\left[S(x_0, x_n)\right] H^{obs}(x_n)}{\sum_n W\left[S(x_0, x_n)\right]}, \tag{5}$$

$$\sigma_H(x_0) = \left\{ \frac{\sum_n W\left[S(x_0, x_n)\right] \left[H^{obs}(x_n) - H(x_0)\right]^2}{\sum_n W\left[S(x_0, x_n)\right]} \right\}^{1/2}, \tag{6}$$

where $H^{obs}(x_n)$ are the observed heat flow values. The weight $W\left[S(x_0, x_n)\right]$ defined by equation (4) can be also considered as the effective number of heat flow measurements at location x_0 deriving from each location x_n. The total effective number of measurements that are applied at each spatial point x_0 is $\sum_n W\left[S(x_0, x_n)\right]$, as shown in Figure 4. There are only a few areas that are very poorly constrained because of unusual crustal or mantle structure; e.g., the Altiplano and Tibet because of anomalously thick crust. Using the effective number of measurements, we also computed local histograms of heat flow at two points in Antarctica, as shown in Figure 5.

The resulting heat flux and standard deviation maps are shown in Figure 6. Low heat flow values are found for old continental regions. Heat flow maximizes on the mid-oceanic ridges and in young tectonically deformed regions. Standard deviations follow the same pattern as the average heat flow; i.e., they minimize in old continental regions and maximize along mid-oceanic ridges and in regions that have undergone relatively recent lithospheric rejuvenation, such as West Antarctica. Figure 7 shows that the standard deviation is almost a linear function of the average heat flow. Large standard deviations are caused by strong small-scale spatial variability in the heat flow data. One of main sources of this variability may be very hydrothermal circulation in the shallow crust. This hydrothermal circulation is more intense in tectonically active regions; i.e., in regions with relatively high average heat flow.

A histogram of the misfit to the data is shown as the solid black line in Figure 8. The fact that the data set is characterized by large spreads caused by substantial

small-scale variability implies that a smooth map will not fit the data very well. The rms-misfit is to the raw data produced by the estimated heat flux map in Figure 6 is 47 mW/m^2. Comparing this with the rms of the data, 55 mW/m^2, demonstrates that the estimated heat flow map reduces the variance in the data only by 27%. Higher variance reductions require much greater local variability in the estimated heat flux.

Discussion

We have presented a method that uses a global seismic model of the crust and upper mantle to extrapolate existing heat flow measurements to regions where such measurements are rare or absent. This method is based on the idea that regions that are structurally similar are expected to have similar levels of heat flow. The structural similarity is quantified by introducing a structural similarity functional. The implementation of the extrapolation technique is non-unique and depends on a number of ad-hoc choices such as the heat flow data set, a particular global seismic model, and on the specific form of the model-based similarity functional and of the corresponding similarity weight function.

An important application of the method presented here is the estimation of expected heat flux for Antarctica, which is needed as input into models of the dynamic evolution of the Antarctic Ice Sheet. The estimated heat-flux map (Figure 6) demonstrates a strong difference between East and West Antarctica with the heat flux almost three times higher in West Antarctica. The elevated level of heat flux may increase the melting rate at the base of the ice and provide more efficient lubrication for fast moving ice streams. This mechanism may contribute to the instability of the West Antarctic Ice Sheet [27, 28, 29]. It should be noted, however, that the heat flux map we have estimated here provides a large-scale average. Small-scale variations caused by variations in hydrothermal circulation, volcanic activity, crustal radioactive heat production, etc. are not present in the estimated maps, but may prove to be very important in modeling the behavior of Antarctic ice streams.

Although our concentration here has been placed on extrapolating heat flow measurements to regions devoid of such information, the method we describe is also useful for interpolation and the production of a smooth global map. For comparison with the estimated heat flux map displayed in Figure 6, Figure 9 shows a heat flow map that has been produced by applying a Gaussian cap (σ = 200 km) spatial smoothing function to the heat flow data of Pollack et al. [1]. The large-scale pattern of the two maps is very similar. Peak values are larger on the map produced by Gaussian smoothing, but this map also looks more 'spotty' and, of course, there are large regions devoid of heat flow values. A comparison between the solid black line and the dashed line in Figure 8 reveals that the map produced by Gaussian smoothing fits the data only a little better than the map estimated by structural similarity. The Gaussian map has an rms-misfit to the raw data of 44 mW/m^2, which is a 36% variance reduction compared with the 27% variance reduction of the estimated heat flux map. The solid grey line in Figure 8 shows that the values in these two heat flow maps are much more similar to each other than they are to the data on which both are based. The rms-misfit between the smoothed data map and the estimated heat flux map is 24 mW/m^2.

Pollack et al. [1] also present a global heat flow map using a degree 12 spherical harmonic representation. There are a number of significant differences between the global estimated heat flux map presented here and Pollack's map. First, Pollack's map predicts much higher heat flow in young oceanic areas. This difference is caused by the fact that we have used the raw heat flow data set both for continents and oceans while Pollack et al. [1] replaced the raw measurements in young oceanic areas with the parametric representation based exclusively on seafloor age [12]. Their purpose was to reduce the influence of measurements biased by hydrothermal circulation through young oceanic crust. The second important difference is that the lateral resolution is higher for the estimated heat flux map presented here due to the fact that the seismic model that guides the structural analogies is higher resolution than spherical harmonic degree 12. The third difference derives from this higher resolution: the maps presented

here are better correlated with continental tectonics. This correlation, in particular, is dramatically improved in Antarctica. We believe that the principal disadvantage of our heat flux maps may be heat flow that is biased toward low values in the young oceans. This bias, however, is not caused by our method but originates in the raw data set. A combination of a cleaned heat flow data base with the method presented in this paper would be likely to produce an unbiased high-resolution global heat flux map.

Global heat flow maps such as that shown in Figure 6 are also useful as constraints to improve future seismic models. Shapiro and Ritzwoller [16] discuss how the assimilation of heat flow data into seismic inversions can improve the seismic model. A major problem is uncertainty in the quality of a global model of heat flow, which the methods discussed in this paper may help to address. The construction of the estimated heat flux map presented here, therefore, can be seen as part of an iterative process in which the seismic model guides the estimation of the global heat flux map which is then fed-back to help refine the seismic model.

Continued improvements in seismic models and further refinements in the heat flow data base will yield better heat flow maps in the future. Discussions are underway toward developing much improved seismic infrastructure on Antarctica which promises great improvements in the resolution of the seismic model across the continent. Application of the estimated heat flux as a basal boundary condition in models of the dynamics of the Antarctic ice sheets will be particularly aided by improvements in the resolution of seismic models across Antarctica.

Acknowledgments. This work was inspired by conversations with Donald Blankenship and Slawek Tulaczyk at the Structure and Evolution of the Antarctic Plate 2003 community workshop in Boulder, CO in early March, 2003. The work was supported by a grant from the US National Science Foundation, NSF-OPP-0125848.

References

[1] H.N. Pollack, S.J. Hurter, J.R. Johnson, Heat flow from the Earth's interior: analysis of the global data set, Revs. Geophys. 31 (1993) 267-280.

[2] N.M. Shapiro, M.H. Ritzwoller, Monte-Carlo inversion for a global shear velocity model of the crust and upper mantle, Geophys. J. Int. 51 (2002) 88-105.

[3] J.L. Bamber, D.V. Vaughan, I. Joughin, Widespread complex flow in the interior of the Antarctic Ice Sheet, Science 287 (2000) 1248-1250.

[4] E. Rignot, R.H. Thomas, Mass balance of polar ice sheets, Science 297 (2002) 1502-1506.

[5] D.D. Blankenship, R.E. Bell, S.M. Hodge, J.M. Brozena, J.C. Behrendt, C.A. Finn, Active volcanism beneath the West Antarctic Ice Sheet and implications for ice-sheet stability, Nature 361 (1993) 526-529.

[6] S. Anandakrishnan, D.D. Blankenship, R.B. Alley, P.L. Stoffa, Influence of sub-glacial geology on the position of a West Antarctic ice stream from seismic observations, Nature 394 (1998) 62-65.

[7] S. Tulaczyk, W.B. Kamb, H.F. Engelhardt, Basal mechanics of Ice Stream B, West Antarctica 2. Undrained plastic bed model, J. Geophys. Res. 105 (2000) 483-494.

[8] A.A. Nyblade, H.N.Pollack, A global analysis of heat flow from Precambrian terrains: implications for the thermal structure of Archean and Proterozoic lithosphere, J. Geophys. Res. 98 (1993) 12,207-12,218.

[9] R.L. Rudnick, W.F. McDonough, R.J. O'Connell, Thermal structure, thickness and composition of continental lithosphere, Chemical Geology 145 (1998) 395-411.

[10] C. Jaupart, J.-C. Mareschal, The thermal structure and thickness of continental roots, Lithos 48 (1999) 93-114.

[11] B. Parsons, J.G. Sclater, An analysis of the variation of ocean floor bathymetry and heat flow with age, J. Geophys. Res. 82 (1997) 803-827.

[12] C.A. Stein, S. Stein, A model for the global variation in oceanic depth and heat flow with lithospheric age, Nature 359 (1992) 123-129.

[13] S.V. Sobolev, H. Zeyen, G. Stoll, F. Werling, R. Altherr, K. Fuchs, Upper mantle temperatures from teleseismic tomography of French Massif Central including effects of composition, mineral reactions, anharmonicity, anelasticity and partial melt, Earth Planet. Sci. Lett. 157 (1996) 193-207.

[14] S. Goes, R. Govers, R. Vacher, R., Shallow mantle temperatures under Europe from P and S wave tomography, J. Geophys. Res. 105 (2000) 11,153-11,169.

[15] A.H.E. Röhm, R. Snieder, S. Goes, J. Trampert, Thermal structure of continental upper mantle inferred from $S-$wave velocity and surface heat flow, Earth Planet. Sci. Lett. 181 (2000) 395-407.

[16] N.M. Shapiro, M.H. Ritzwoller, Thermodynamics constraints on seismic inversions, Geophys. J. Int. in press.

[17] M.H. Ritzwoller, A.L. Levshin, Eurasian surface wave tomography: Group velocities, J. Geophys. Res. 103 (1998) 4839-4878.

[18] M.H. Ritzwoller, N.M. Shapiro, A.L. Levshin, G.M. Leahy, The structure of the crust and upper mantle beneath Antarctica and the surrounding oceans, J. Geophys. Res. 106 (2001) 30645-30670.

[19] J. Trampert, J.H. Woodhouse, J.H., Global phase velocity maps of Love and Rayleigh waves between 40 and 150 s period, Geophys. J. Int. 122 (1995) 675-690.

[20] G. Ekström, J. Tromp, E.W.F. Larson, Measurements and global models of surface waves propagation, J. Geophys. Res. 102 (1997) 8137-8157.

[18] M.H. Ritzwoller, N.M. Shapiro, M.P. Barmin, A.L. Levshin, Global surface wave diffraction tomography, J. Geophys. Res. 107 2335 (2002) ESE 4-1 - 4-13.

[22] I.W.D. Dalziel, Antarctica; A tale of two supercontinents? Annu. Rev. Earth Planet. Sci. 20 (1992) 501-526.

[23] W.A.,Gose, M.A. Helper, J.N. Connelly, F.E. Hutson, I.W.D. Dalziel, Paleomagnetic data and U-Pb isotopic age determinations from Coats Land, Antarctica: Implications for late Proterozoic plate reconstructions, J. Geophys. Res. 102 (1997) 7887-7902.

[24] W.E. LeMasurier, Late Cenozoic volcanism on the Antarctic Plate – An overview, in *Volcanoes of the Antarctic Plate and Southern Oceans AGU, Antarctic Research Series*, edited by LeMasurier, W. E. and Thomson, J. W., 48 (1990) pp. 1-17.

[25] J.C. Behrendt, C.A. Finn, D.D. Blankenship, R.E. Bell, Aeromagnetic evidence for a volcanic caldera(?) complex beneath the divide of the West Antarctic Ice Sheet, Geophys. Res. Lett. 25 (1998) 4385-4388.

[26] J.C. Behrendt, Crustal and lithospheric structure of the West Antarctic Rift System from geophysical investigations - a review, Global and Planetary Change 23 (1999) 25-44.

[27] R. Bindschadler, Future of the West Antarctic Ice Sheet, Science 282 (1998) 428-429.

[28] M. Oppenheimer, Global warming and the stability of the West Antarctic Ice Sheet, Nature 393 (1998) 325-331.

[29] R.P. Sherer, A. Aldahan, S. Tulaczyk, G. Possnert, H. Engelhardt, B. Kamb, Pleistocene collapse of the West Antarctic Ice Sheet, Science 281 (1998) 82-85.

N.M. Shapiro and M.H. Ritzwoller

Center for Imaging the Earth's Interior

Department of Physics, University of Colorado

Boulder, CO 80309-0390, USA

(e-mail: nshapiro@ciei.colorado.edu)

Received ; revised ; accepted .

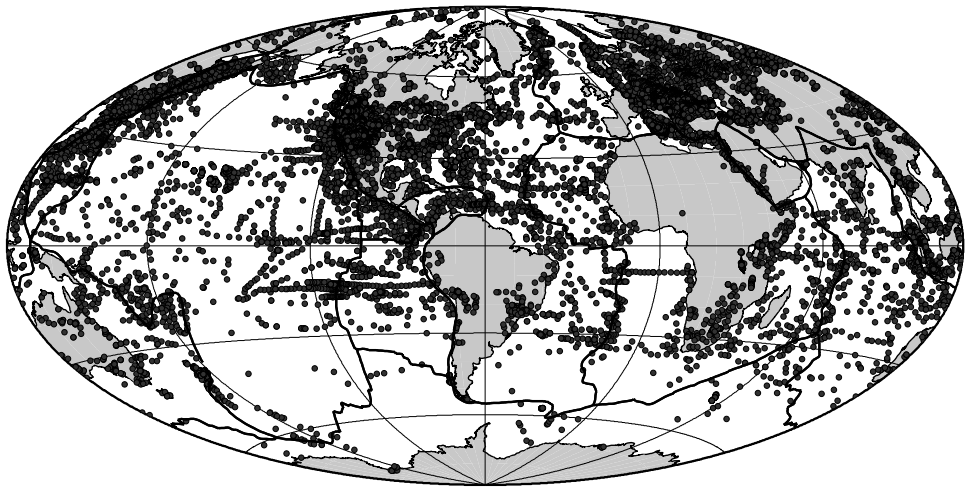

Figure 1. Distribution of the heat flow data from the database of Pollack et al. [1]. Here and after, thick black lines show the plate boundaries.

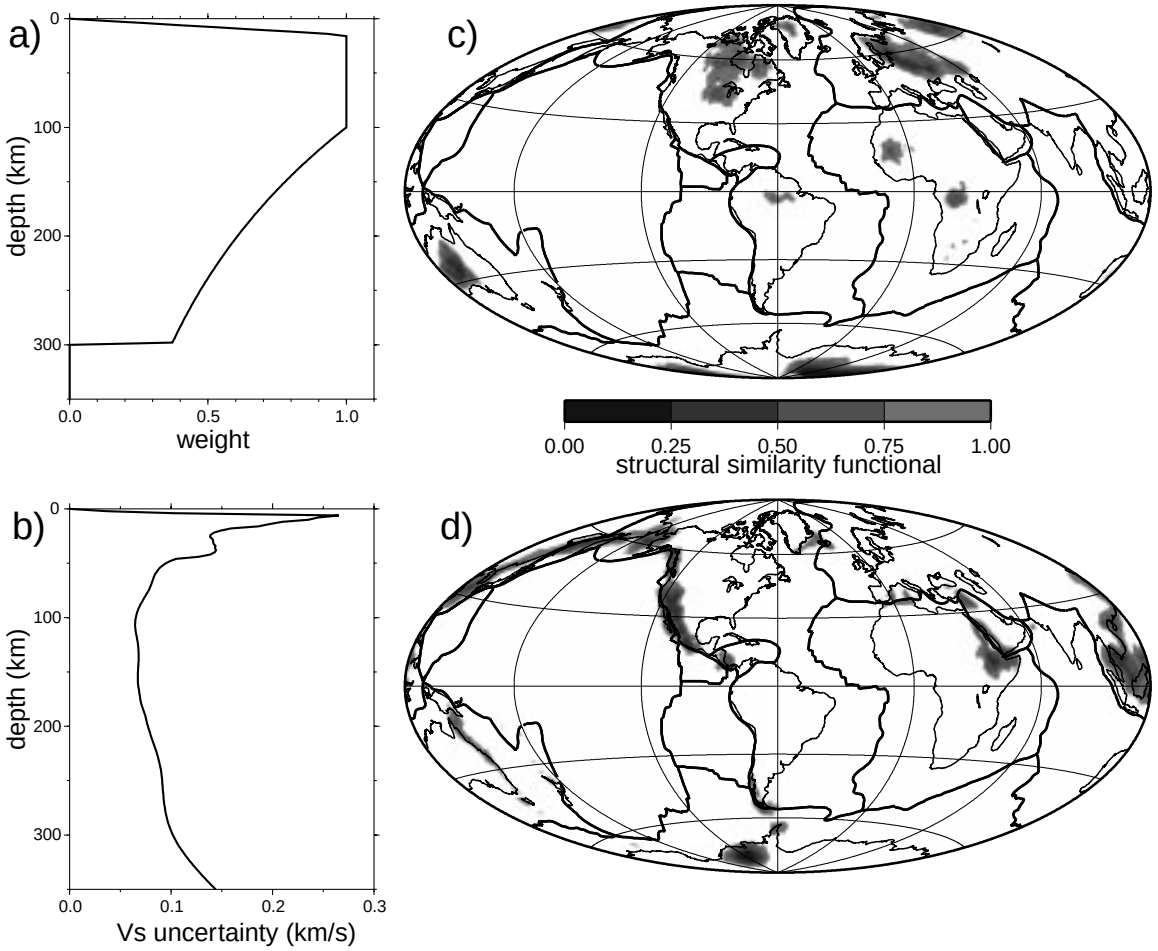

Figure 2. (a) Weights $w(z)$ used in equation (2) to define the structural similarity functional. (b) Model uncertainty $u(z)$ used in equation (2). (c) Distribution of the similarity functional with respect to a location in East Antarctica (84S, 90E). (d) Distribution of the similarity functional with respect to a location in West Antarctica (78S, 110W).

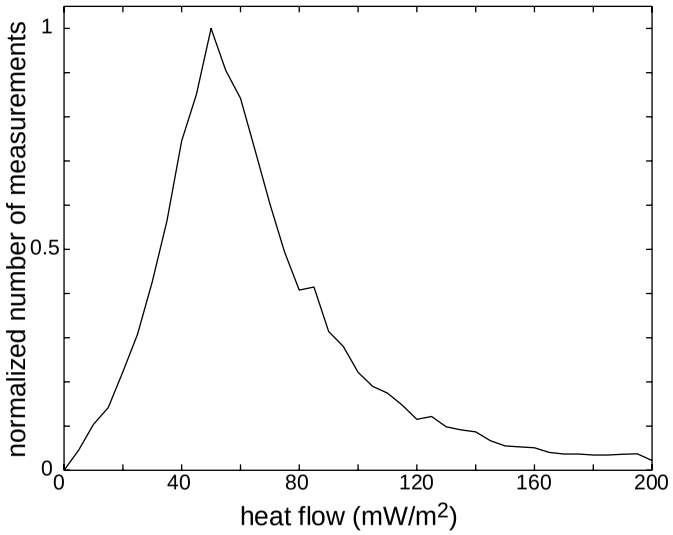

Figure 3. Histogram of heat flow values from the data base of Pollack et al. [1].

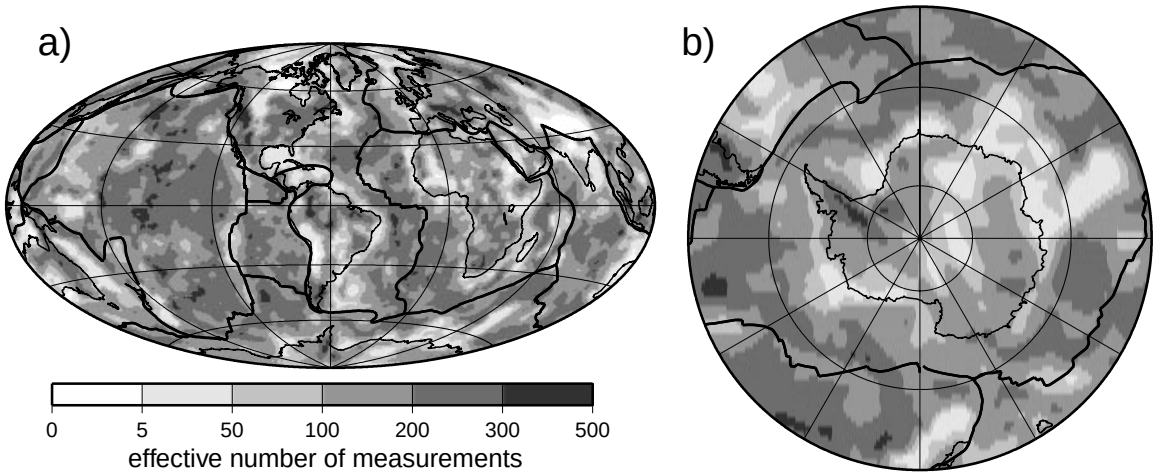

Figure 4. Effective number of heat flow measurements applied at each spatial point, $\sum_n W\left[S(x_0, x_n)\right]$.

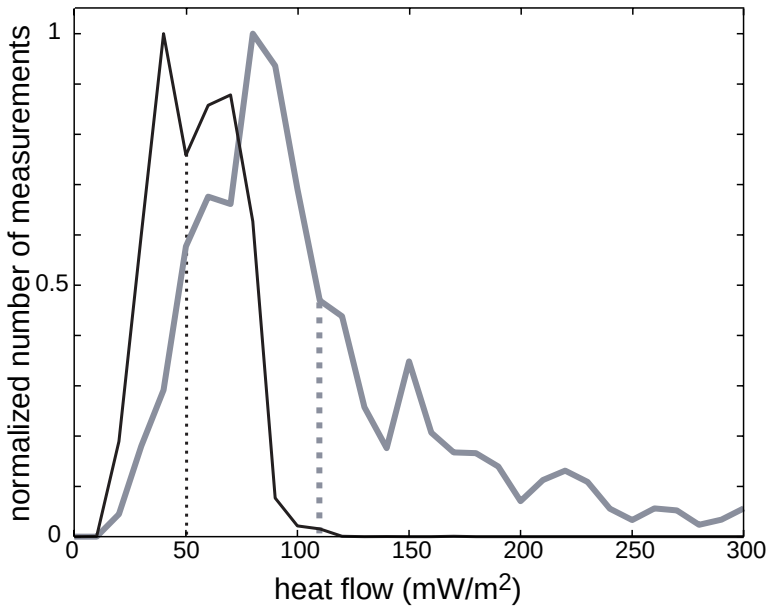

Figure 5. Histograms of surface heat flux computed using the similarity-based weight function ($W\left[S(x_0, x_n)\right]$ as the effective number of heat flow measurements at two values of x_0: (Black Line) a point in East Antarctica (84S, 90E) and (Grey Line) a point in West Antarctica (78S, 110W). The average of each distribution, identified by the dotted lines, define the estimated heat flux at each spatial point.

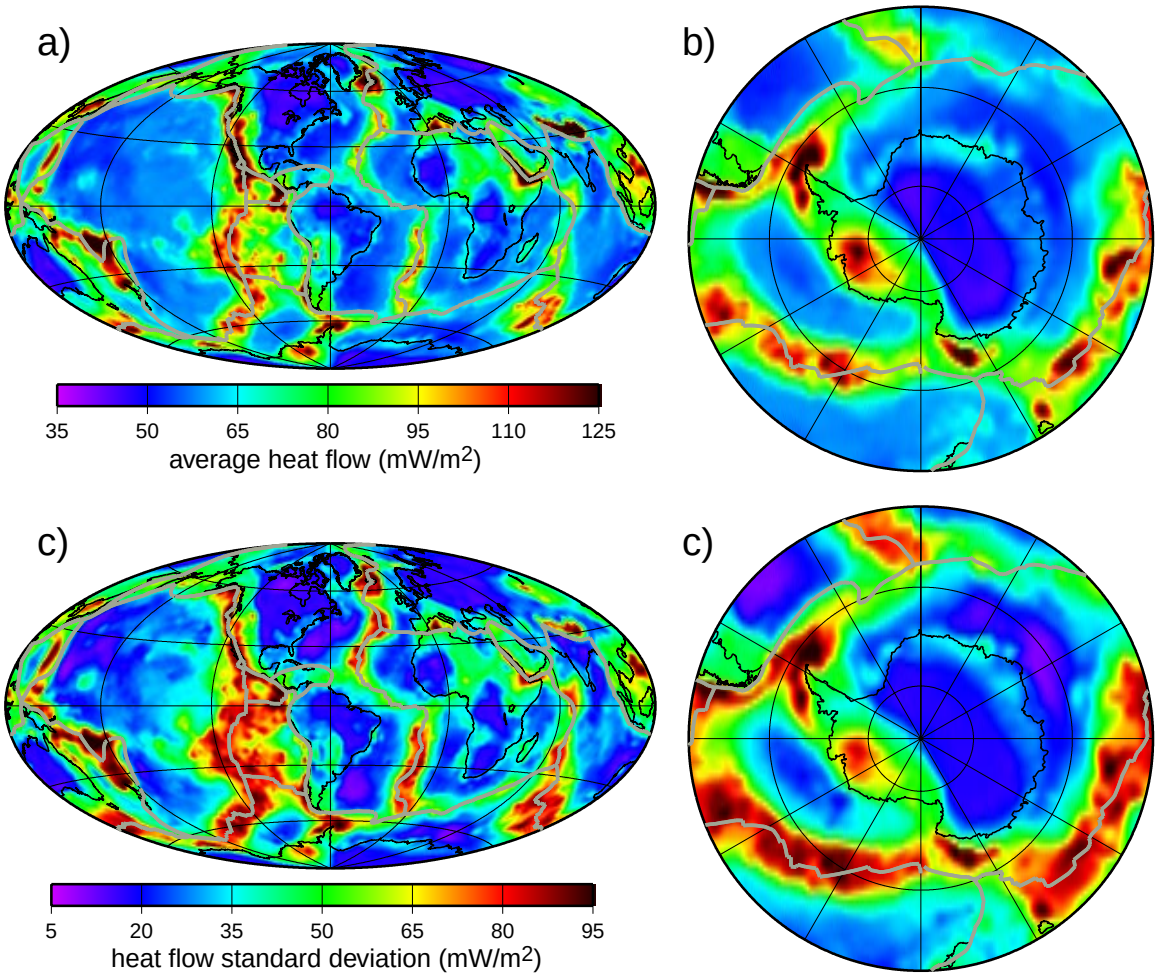

Figure 6. (a) and (b) Estimated heat flux produced by equation (5). (c) and (d) Standard deviation of the distribution of heat flow measurements used at each point, produced by equation (6), respectively.

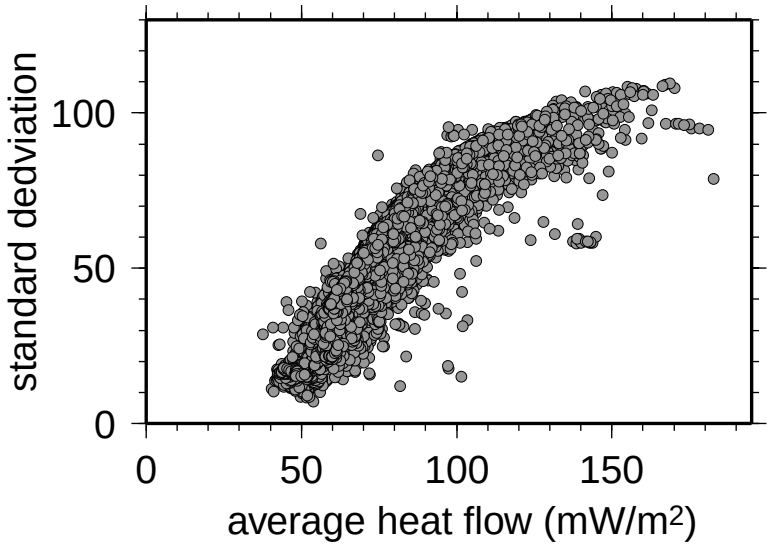

Figure 7. Standard deviation of heat flux obtained using equation (6) plotted as function of the average taken from equation (5) for all points on a $2^\circ \times 2^\circ$ global grid.

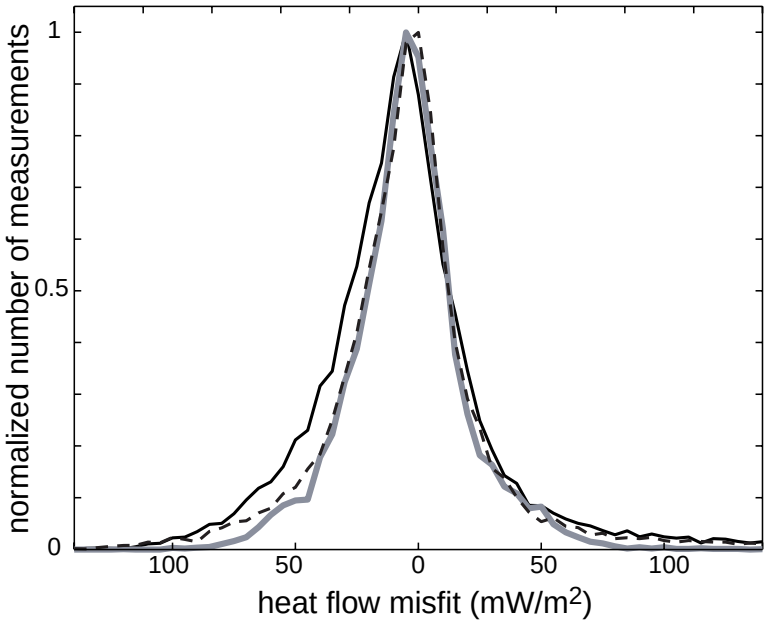

Figure 8. (Solid Black Line) Histogram of the misfit between the raw data and the estimated heat flux shown in Figure 6. (Dashed Line) Histogram of the misfit between the raw data and the heat flow values found by spatially smoothing the raw data, as shown in Figure 9. (Solid Grey Line) Histogram of the misfit between the values in the smoothed data map shown in Figure 9 and the estimated heat flow values shown in Figure 6.

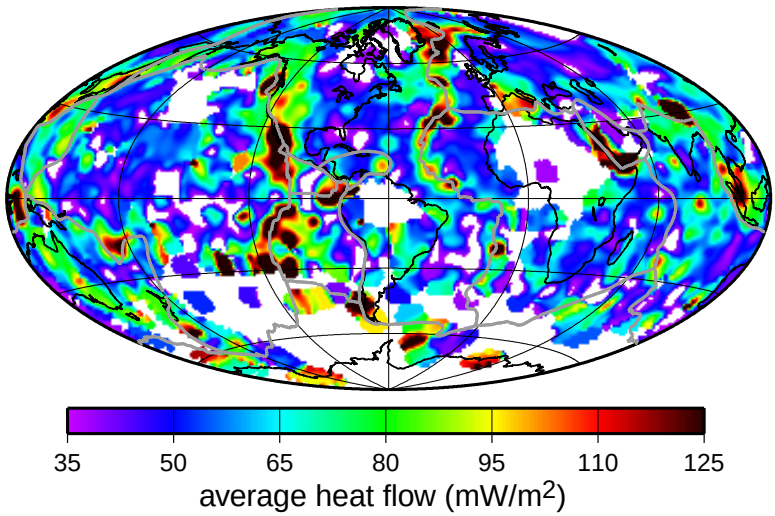

Figure 9. Heat flow map obtained by applying a Gaussian cap (σ = 200 km) spatial smoothing function to the data of Pollack et al. [1]. The white regions identify the areas devoid of measurements.